Advanced Materials Interfaces

Substrate Selection for Full Exploitation of Organic Semiconductor Films: Epitaxial Rubrene on B-alanine Single Crystals

--Manuscript Draft--

Manuscript Number:	
Full Title:	Substrate Selection for Full Exploitation of Organic Semiconductor Films: Epitaxial Rubrene on B-alanine Single Crystals
Article Type:	Full Paper
Keywords:	rubrene; organic epitaxy; b.alanine; crystalline thin films; wet-transfer.
Corresponding Author:	Silvia Trabattoni, Ph.D. University of Milano-Bicocca Milan, ITALY
Additional Information:	
Question	**Response**
Corresponding Author Secondary Information:	
Corresponding Author's Institution:	University of Milano-Bicocca
Corresponding Author's Secondary Institution:	
First Author:	Silvia Trabattoni, Ph.D.
First Author Secondary Information:	
Order of Authors:	Silvia Trabattoni, Ph.D.
	Luisa Raimondo, PhD
	Marcello Campione, PhD
	Daniele Braga, PhD
	Vincent C. Holmberg, PhD
	David J. Norris
	Massimo Moret, PhD
	Andrea Ciavatti, PhD
	Beatrice Fraboni
	Adele Sassella, PhD
Order of Authors Secondary Information:	
Abstract:	Rubrene (RUB) is one of the most studied organic semiconductors because, in the orthorhombic single-crystal phase, it exhibits record exciton diffusion length and one of the highest charge carrier mobility ever reported. Here, thin films of oriented crystalline RUB are successfully grown in vacuum on millimeter-sized (010)-β-alanine (β-ala) single crystals with a step-growth protocol, exploiting organic epitaxy. The experimental characterization demonstrates that these RUB films grow in the orthorhombic polymorph with the (100)RUB plane in contact with the (010)β-ala surface and with precise azimuthal orientations. A complementary study of the RUB(100)/β-ala(010) interface, performed by computational simulations, confirms the epitaxial relations expected by considering the molecular scale corrugations of the surfaces. Moreover, thanks to the wide transparency region of β-ala, the RUB absorption bands in the UV range are directly detected for the first time. Finally, removal of the water-soluble substrate enables the integration of the films in field effect transistors as high quality active organic layers. The characteristics of such RUB-based devices confirm the

	quality and versatility of epitaxial thin films for organic electronics.

WILEY-VCH

DOI: 10.1002/ ((please add manuscript number))
Article type: Full Paper

Substrate Selection for Full Exploitation of Organic Semiconductor Films: Epitaxial Rubrene on β-alanine Single Crystals

*Silvia Trabattoni *, Luisa Raimondo, Marcello Campione, Daniele Braga, Vincent C. Holmberg†, David J. Norris, Massimo Moret, Andrea Ciavatti, Beatrice Fraboni, Adele Sassella*

Dr. S. Trabattoni, Dr. L. Raimondo, Prof. Dr. M. Moret, Prof. Dr. A. Sassella
Department of Materials Science, University of Milano Bicocca, via Cozzi 55, 20125 Milan, Italy
E-mail: silvia.trabattoni@mater.unimib.it

Dr. M. Campione
Department of Earth and Environmental Sciences, University of Milano Bicocca, piazza della Scienza 4, 20126 Milan, Italy

Dr. D. Braga, Prof. Dr. V. C. Holmberg, Prof. Dr. D. J. Norris
Optical Materials Engineering Laboratory, ETH Zürich, 8092 Zürich, Switzerland

Dr. A. Ciavatti, Prof. Dr. B. Fraboni
Department of Physics and Astronomy, University of Bologna, viale Berti-Pichat 6/2, 40127 Bologna, Italy

Keywords: rubrene, organic epitaxy, β-alanine, crystalline thin films, wet-transfer

Rubrene (RUB) is one of the most studied organic semiconductors because, in the orthorhombic single-crystal phase, it exhibits record exciton diffusion length and one of the highest charge carrier mobility ever reported. Here, thin films of oriented crystalline RUB are successfully grown in vacuum on millimeter-sized (010)-β-alanine (β-ala) single crystals with a step-growth protocol, exploiting organic epitaxy. The experimental characterization demonstrates that these RUB films grow in the orthorhombic polymorph with the $(100)_{RUB}$ plane in contact with the $(010)_{\beta\text{-ala}}$ surface and with precise azimuthal orientations. A complementary study of the RUB(100)/β-ala(010) interface, performed by computational simulations, confirms the epitaxial relations expected by considering the molecular scale

corrugations of the surfaces. Moreover, thanks to the wide transparency region of β-ala, the RUB absorption bands in the UV range are directly detected for the first time. Finally, removal of the water-soluble substrate enables the integration of the films in field effect transistors as high quality active organic layers. The characteristics of such RUB-based devices confirm the quality and versatility of epitaxial thin films for organic electronics.

1. Introduction

Organic semiconducting materials (small molecules, oligomers, and polymers) receive great attention for applications in optoelectronics and they are now employed successfully in devices such as organic light emitting diodes (OLEDs). In contrast, performances of organic field effect transistors (OFETs) and organic solar cells are still limited, because the charge transport properties of the organic active layers are heavily affected by local disorder. Among organic molecular semiconductors, rubrene (5,6,11,12-tetraphenyltetracene, RUB) is a benchmark material which, in the orthorhombic single-crystal phase, shows exciton diffusion lengths of several micrometers and charge carrier mobilities as high as 20 $cm^2 V^{-1} s^{-1}$.[1–3] The exploitation of RUB thin films instead of single-crystals could be useful to overcome problems related to poor thickness and lateral size control that hinder single-crystal integration in optoelectronic devices. However, the integration of RUB thin films is strictly influenced by their crystalline quality in terms of crystalline domain coherence and orientation, since RUB charge transport properties may be limited by grain boundaries and are anisotropic.[1] Moreover, when deposited by conventional vacuum techniques, RUB forms amorphous thin films on a wide variety of substrates,[4,5] therefore exhibiting poor electrical properties. In the literature, many works report different deposition vacuum techniques[6,7] and approaches (i.e. epitaxial growth, buffers layers,[8–10] and/or post-growth treatments[11,12]) tested to enhance the film quality and, thus, to improve OFET performances. For example, the

weak epitaxy growth introduced by Yan et al.[13,14] and the epitaxy on van der Waals surfaces[15,16] allow to deposit RUB films directly on dielectric substrates, but only exploiting organic epitaxy the best outcomes in terms of crystalline quality have been achieved.[17–20] The proper substrate choice stimulates the epitaxial growth of RUB thin films with a unique orientation,[19,21,22] even if successful integration into the devices may be hardly achieved. Therefore, the most suitable substrates are those which possess both the ability in driving the growth of crystalline films, possibly displaying a unique azimuthal orientation, and the suitable characteristics for device integration.

In this work, we have selected an amino acid single-crystal substrate, namely (010)-β-alanine (β-ala),[23] having already been exploited to induce a preferential orientation in other organic overlayers.[24] These crystals are easy to grow in solution and they are highly water-soluble,[25] allowing for the wet-transfer[26,27] of the epitaxial films deposited on them. We have studied extensively the interface between β-ala(010) substrates and crystalline RUB films, grown by organic molecular beam epitaxy (OMBE) at room temperature without any post-growth treatments. These millimeter-sized, crystalline, and oriented RUB thin films have been fully characterized by X-ray diffraction (XRD), atomic force microscopy (AFM), UV-visible spectroscopy, transmission electron microscopy (TEM), and selected-area electron diffraction (SAED), determining the structure and orientation of the film and the epitaxial relation with β-ala(010), rationalized in terms of surface corrugation match. Experimental results have been also successfully compared to computational simulations of the RUB/β-ala interface. Eventually, the choice of β-ala(010) has been definitively demonstrated to be good also for RUB device integration. Indeed, thanks to the wet-transfer of RUB thin films displaying controlled thickness and size onto a dielectric substrate, we have fabricated working OFETs, achieving mobility up to 2 $cm^2 V^{-1} s^{-1}$.

2. Results and discussion

2.1 RUB thin film characterization. RUB thin films grow on β-ala(010) in layered islands, which completely cover the substrate surface at thicknesses above ≈5 nm. In **Figure 1a and 1b**, AFM images of 5 nm and 50 nm thick films are shown, respectively. Layers with a uniform step height of 1.35±0.04 nm are clearly visible in the cross-sectional profile reported in Figure 1a. The thicker film is composed by elongated pseudo-hexagonal features with polygonal edges and a pyramidal morphology, with the same step height. Such features run mainly parallel to two directions, symmetric with respect to the $[001]_{\beta\text{-ala}}$ axis, highlighted by the white arrows in Figure 1b. The out-of-plane film structure was analyzed by XRD specular scans, after films were wet-transferred onto Si(100) substrates. The results are shown in **Figure 1c** for two film thicknesses. The *h00* reflections of the orthorhombic polymorph of RUB[28] are visible, demonstrating the crystallinity of both films and complete textural order, with the $(100)_{RUB}$ plane in contact with $(010)_{\beta\text{-ala}}$. (For a comparison with single-crystal XRD patterns, see Supporting Information Figure S1). The (200) planes enclose monomolecular layers with a 1.34 nm spacing, in accordance with the step height measured by AFM.

To get further insight into the macroscopic properties of RUB thin films, optical absorption spectra were collected in the UV-visible range, where the characteristic absorption bands of RUB are usually observed. **Figure 2a** shows normal incidence spectra, in the range from 2.0 to 3.2 eV, collected on ≈3 mm^2 area on a 5 nm thick RUB film grown on β-ala(010), with the electric field parallel to $[100]_{\beta\text{-ala}}$ (full line) and $[001]_{\beta\text{-ala}}$ (dotted line). These are the spectra that show the strongest difference, when the dependence of the thin film absorption on the polarization direction of the incident light is considered. **Figure 2b** reports analogous spectra for a (100)-oriented orthorhombic RUB single crystal, collected with the electric field parallel to $[001]_{RUB}$ (full line) and $[010]_{RUB}$ (dotted line). The spectra of the RUB thin film reproduce the single crystal spectra in terms of peak positions and lineshape for different polarizations, giving full evidence of the crystallinity of the film on a macroscopic area and of its

preferential orientation with $[010]_{RUB}$ aligned with $[001]_{\beta\text{-ala}}$. Oblique incidence transmission measurements on the thin film (dashed spectrum in Figure 2a) show a strong, low energy peak at about 2.35 eV (it is absent in all the other spectra in Figure 2, where only the known shoulder at 2.32 eV is present[29]). This absorption peak originates from a transition polarized parallel to the $[100]_{RUB}$ axis,[29] providing additional evidence that the $(100)_{RUB}$ plane is parallel to the film surface, in full agreement with the results obtained with the AFM and diffraction experiments. Thanks to the wide UV-vis transparency region of β-ala, to the crystallinity of the films, and to their low thickness, the absorption spectra of crystalline RUB at energy higher than 4 eV can also be directly detected. **Figure 2c** shows spectra up to 5.3 eV, acquired at normal incidence on the same films, with the polarization of the incident light varying from 0° (electric field parallel to $[100]_{\beta\text{-ala}}$) to 90° (electric field parallel to $[001]_{\beta\text{-ala}}$). The peak at 3.73 eV shows its maximum intensity for the electric field parallel to $[100]_{\beta\text{-ala}}$, then it decreases gradually, as well as the peak at 4.12 eV, by changing the light polarization direction; at the same time, the peaks at 3.98 and 4.30 eV raise and they become the most intense ones when the electric field is parallel to $[001]_{\beta\text{-ala}}$. The corresponding high energy transitions have very high oscillator strength (1-2 order of magnitude higher than RUB transitions in the visible spectral range), and this is why they can be detected only for very thin single crystals. In the literature, for example, absorption spectra of crystalline RUB are reported only up to 4.1 eV.[20,22] Thus, this is the first time the complete optical absorption of crystalline RUB is reported, with intensity and peak positions in agreement to those deduced by regression of ellipsometry data acquired on RUB single crystals.[29] In conclusion, from the macroscopic optical characteristics, our RUB thin films are to be considered as extremely thin RUB single crystals lying on β-ala with $(100)_{RUB}$ as contact plane and the $[010]_{RUB}$ direction aligned with $[001]_{\beta\text{-ala}}$.

By wet-transferring a RUB film onto a carbon-coated copper TEM grid, bright-field images were collected (**Figure 3a**), in which domains with dominant elongation parallel to the two

directions indicated by the red arrows are visible. The azimuthal order of the films was evaluated by the SAED pattern displayed in **Figure 3b**. Clear diffraction spots are distributed in accordance to the superposition of two patterns corresponding to two (100)-oriented domains of the orthorhombic polymorph, azimuthally rotated by 26.5°, matching the orientation of the elongations observed in Figures 1b and 3a, with the RUB preferential growth direction parallel to $[010]_{RUB}$.

In order to map the distribution of domains orientations, an apertured dark-field TEM analysis was also performed. The TEM images in **Figure 4** display the spatial distribution of the two domain orientations within the RUB thin film. When one set of diffraction spots is selected, the domains corresponding to that particular orientation appear bright, and when diffraction spots from the other orientation are selected, the other set of domains rotated by 26.5° lights up. As can be seen in Figure 4b and 4c, the domains observed have similar size, and both orientations appear with nearly equal weight. The equally probable occurrence of the two orientations can also be deduced from the symmetric intensity distribution of the diffraction spots in Figure 3b. It should be noted that, due to the large lattice parameter of RUB, the diffraction spots are very closely packed in reciprocal space; therefore, it was not possible to completely exclude all of the diffraction spots from one orientation, even using the smallest available aperture. Nevertheless, by positioning the aperture such that a majority of diffraction spots from one orientation was selected, it was still possible to get reliable results on the spatial distribution of the two orientations (see Supporting Information Figure S2). The results of the structural characterization performed locally with TEM have been confirmed on a global scale by grazing incidence X-ray diffraction (GIXD) with synchrotron radiation, as discussed in Supporting Information Figure S3 and S4.

2.2 Microscopic Model of the Interface. Following established arguments of organic epitaxy, the azimuthal ordering of RUB films on β-ala(010) can be rationalized. We have already

pointed out[30–33] that the orientation mechanism for building organic hetero-interfaces is dictated by molecular scale corrugations of the involved crystalline surfaces. The β-ala(010) cleavage surface is lined up with pairs of H atoms of the aliphatic molecular backbone running parallel to the $[100]_{\beta\text{-ala}}$ axis (**Figure 5a**); this surface structure gives rise to wavy grooves running parallel to <101> directions with a spacing of 5.18 Å. On the other hand, the $(100)_{RUB}$ surface is lined up with phenyl H atoms defining trenches along <021> directions with a spacing of 5.08 Å (**Figure 5b**). The mismatch of 1.9% between these two directions is the lowest ever encountered in the framework of organic-organic epitaxy. The alignment of RUB domains in accordance with this line-on-line epitaxial relation[34] gives rise to two couples of symmetrically equivalent domains with the unit cell rotated by exactly 26.5° (±13.25° to $[001]_{\beta\text{-ala}}$ and ±13.25° to $[100]_{\beta\text{-ala}}$); for clarity, in Figure 5a only the couple of domains at ±13.25° to $[001]_{\beta\text{-ala}}$ is reported.

The investigation of energy landscape with properly selected intermolecular potentials can provide a more robust rationalization of observed epitaxial relations.[33,35,36] Moreover, symmetry arguments determine the number of equivalent isoenergetic orientations to be found on a substrate.[24,30,37] The β-ala(010) cleavage surface (plane group symmetry *pg*) owns glide lines parallel to $[100]_{\beta\text{-ala}}$. Hence, crystallites with azimuth θ have isoenergetic symmetric counterparts at 180°-θ, when defining θ = 0° along $[001]_{\beta\text{-ala}}$. Similarly, $(100)_{RUB}$ islands maintain binary rotational symmetry (C_2), implying reduction of the configuration space to 0-180°.

In **Figure 6**, results of force-field simulations describe the average adhesion energies per overlayer molecule of the RUB(100)/β-ala(010) interface as a function of azimuth θ (angle between $[010]_{RUB}$ and $[001]_{\beta\text{-ala}}$). The adhesion energy scatterplot shows favorable azimuthal configurations at θ = 11.8° and 75.5° (and their symmetry equivalent orientations at 168.2° and 104.5°, naturally arising from the genetic algorithm sampling). The average adhesion energy per molecule amounts to ≈ −34 kJ mol^{-1} for all four azimuths, indicating there should

be no preference between the two groups of orientations. The experimental epitaxial relation, i.e. the two main domain orientations observed by AFM and TEM differing by ≈ 26.5°, is coherent only with the interface model with θ ≈ 12/168°. The other calculated epitaxial relation with θ ≈ 75/105° is experimentally confirmed by very low intensity peaks in GIXD measurements (see Supporting Information Figure S4), it appears very rarely in AFM images of thick films and it is not detected in the sample areas analyzed by TEM. The couple of domains oriented at θ ≈ 12/168° appears therefore to be kinetically preferred with respect to nuclei with θ ≈ 75/105°, whereas they should be observed with the same statistical frequency, being energetically equivalent. All heteroepitaxial systems previously analyzed with the same computational approach[19,20,24,30,38] never showed such a discrepancy, always providing a good semi-quantitative accordance between observed azimuthal orientations and their mass abundance in the grown OMBE films according to Boltzmann's statistical weight. In the present case, the difference in the repeating pattern at molecular scale along $[100]_{\beta\text{-ala}}$ or $[001]_{\beta\text{-ala}}$ directions could be large enough to suppress almost entirely the growth of two-dimensional RUB(100) nuclei corresponding to azimuth θ ≈ 75/105°. It is worth noting that also the macroscopic orientation deduced by optical spectroscopy (the $[010]_{RUB}$ axis aligned with $[001]_{\beta\text{-ala}}$) is in agreement with the inferred epitaxial relation with θ ≈ 12/168°, therefore further confirmed to be the preferred one. Indeed, the two domains display equal weight and are symmetrically-oriented with respect to β-ala axes. Moreover, a misalignment as small as ±13.25° would not be detectable in the UV-visible spectra for such low film thicknesses.

2.3 Device fabrication and electrical characterization. In order to assess the quality of RUB thin films for electronic applications, we fabricated bottom-gate/top-contact OFETs with Cytop as the insulating layer, sketched in **Figure 7a**. Our strategy for producing transferable/free-standing RUB thin films overcomes the limits imposed by the high

hydrophobicity of Cytop in back-gated OFET, where the active layer has to be deposited on top of the dielectric.[39]

Figure 7b shows the dependence of the drain current (I_D) of a RUB-based OFET on the drain voltage (V_D), at different gate voltages (V_G) (output characteristics). The characteristics show ideal OFET behavior: at low V_D the current increases linearly with the applied drain voltage and saturates at $V_D \approx V_G$, as expected for a long-channel OFET with negligible contact effects. Moreover, the characteristics are nearly hysteresis-free, indicating a reduced effect of charge trapping at the insulator/semiconductor interface, as for single-crystal OFETs employing Cytop as an insulator.[40] Also, a negligible hysteresis is seen in the transfer characteristics (I_D-V_G) of OFET at different drain voltages (**Figure 7c**). However, the trend of the I_D-V_G characteristics deviates from the ideal behavior observed in RUB single-crystal transistors.[41] In the linear (black curve, V_D = -5 V) and saturation (blue curve, V_D = -35 V) regimes, a substantial decrease of the slope is observed at high gate voltages, after the initial increase in the linear and parabolic I_D-V_G regimes. This behavior has previously been attributed to the contribution of the parasitic resistance of the contacts[42,43] or to the dependency of the mobility on the gate voltage.[44,45] Both these issues are well-known and widely-documented bottlenecks for the development of OFETs.

To avoid incorrect extraction of the charge carrier mobility μ (due to incorrect determination of the threshold voltage V_T), the mobility was extracted from the characteristics of devices working in saturation and at the peak of the derivative of the $(I_D)^{½} \sim \mu^{½}(V_G-V_T)$ characteristics. RUB-based OFETs show reasonably high charge carrier mobility (1 to 2 cm^2 V^{-1} s^{-1} values were obtained for different devices, as summarized in Supporting Information Table 1), together with other satisfactory parameters, such as a low threshold voltage (-2 V < V_T < +6 V), an ON/OFF ratio of about 10^4 at ±15 V from V_T in the saturation regime (see Supporting Information Figure S6), and a normalized subthreshold swing[46] S as low as 17 V nF dec^{-1} cm^{-2}.

3. Conclusion

In summary, we have demonstrated that millimeter-sized, crystalline, oriented thin films of orthorhombic RUB can be obtained by OMBE, exploiting organic epitaxy and working at room temperature without post-growth treatments. The key is the selection of an organic crystalline substrate enabling the growth of RUB epitaxial overlayer. In the present case, β-ala(010) surface corrugations have displayed a surprising match with those of orthorhombic RUB giving rise to the best accordance in terms of line-on-line epitaxial relation ever encountered in the framework of organic-organic epitaxy. Despite the relatively high symmetry of β-ala surface, kinetic factors select just one couple of equivalent azimuthal orientations, thus allowing for the growth of highly oriented RUB films. The wide transparency spectral range of β-ala has allowed to detect directly the RUB absorption bands in the UV range that much more characterize the optical anisotropy of crystalline RUB. Moreover, thanks to the high water solubility of β-ala, transferable/free-standing RUB films were obtained and integrated in working OFET fabricated with Cytop as dielectric.

In conclusion, we have demonstrated that a careful selection of the substrate is the key i) to obtain highly crystalline and oriented films with controlled size and thickness, even in the case of molecules with a strong tendency in forming amorphous overlayers, like RUB, ii) to address the intrinsic properties of organic semiconductor directly, and iii) to obtain transferable crystalline films for devices integration.

4. Experimental Section

Materials and Methods. β-ala was purchased from Sigma-Aldrich. Single crystals were grown from supersaturated water solutions at 30 °C following procedures previously described.[24] Centimeter-sized single crystal β-ala(010) substrates were freshly cleaved just before introduction into the deposition chamber. RUB powder was purchased from Acros Organics.

All RUB thin films were grown by OMBE under ultra-high vacuum (pressure $\leq 5\times10^{-9}$ mbar), using Knudsen-type effusion cells, while the thickness was monitored in-situ with a quartz microbalance. A two-step growth protocol was employed, similar to what is sometimes used to improve the structural quality of inorganic thin films and heterostructures;[47] two-step growth is also known to enable spontaneous ordering in organic materials.[22,48] The OMBE growth was interrupted after the deposition of the first few molecular layers (first step), the sample was kept in vacuum, and the process was then resumed to obtain the desired thickness (second step), namely 3 - 100 nm. The deposition temperature was 185 °C, with a growth rate of less than 1 Å min^{-1}, and 200 °C, with a growth rate of 4 Å min^{-1}, for the first and second deposition steps, respectively. RUB single crystals to be used as a reference were grown by physical vapor transport in a horizontal tube 75 cm long placed in a three-zone furnace with a temperature gradient of 2 °C cm^{-1} and a nitrogen flux of 50 mL min^{-1}.

Characterization. The surface morphology of the films was analyzed by AFM using a Bruker Nanoscope V in intermittent-contact mode in air with silicon probes (force constant 20-80 N m^{-1} and resonance frequency 287-346 kHz). XRD experiments were performed by recording specular scans (θ/2θ mode) with a Panalytical X'Pert Pro powder diffractometer in the Bragg-Brentano parafocusing geometry, using Cu Kα radiation (λ = 1.54 Å). Optical transmission was measured on ≈3 mm^2 sample regions in the spectral range from 2 to 6 eV with a Perkin Elmer Lambda 900 instrument at normal and oblique incidence under polarized light, using Glan-Taylor calcite polarizers. Samples for TEM analysis were prepared by transferring free-standing RUB thin films onto carbon-coated 200-mesh copper-foil TEM grids (Plano GmbH). TEM characterization and selected-area electron diffraction (SAED) were performed on a Philips CM12 transmission electron microscope operating at 100 kV. Apertured dark-field TEM images were collected using a FEI Tecnai F30 TEM operating at 300 kV.

Computational Methods. Energetically feasible epitaxial relationships were investigated by means of Lamarckian genetic algorithms as implemented in the AutoDock3 package,[49]

following a successful procedure used for several organic-organic[19,20,24,30,33,35,38] and organic-inorganic heteroepitaxial systems.[36] The configuration space, represented by the azimuthal angle between rigid substrate and overlayer, has been explored for a bulk terminated β-ala(010) slab comprising 12 × 2 × 20 unit cells along *a*, *b*, and *c* directions,[23] respectively, for a total of 3822 β-ala molecules. One molecule thick slices of the overlayer, comprising 16 or 51 molecules, were used in 2048 docking runs for randomly oriented overlayer islands, moving freely above the substrate. Potential energy maps were evaluated over 351^3 grid points spaced by 0.22 Å with the OPLS all-atom empirical potential for description of intermolecular interactions.[50,51] Energy minima configurations found with Autodock were fully optimized with the same force field by using program Orient (version 4.8.06)[52] with a substrate of 17 x 3 x 27 unit cells along *a*, *b*, and *c* directions, respectively, starting with five different configurations for each of the four azimuthal orientations with good adhesion energy.

Device Fabrication. Bottom-gate/top-contact RUB OFETs were fabricated in air or under dry N_2 atmosphere. The insulating fluoropolymer Cytop[40] was deposited by spin-coating onto a clean ITO-coated glass substrate (Cytop CTL-809M, Asahi Glass; 270 to 400 nm final thickness), followed by thermal annealing (30 min at 90 °C and 30 min at 120 °C), in air. RUB thin films (thickness of 50 nm) on β-ala substrates were placed upside-down onto the ITO/Cytop gate electrode; the slow and controlled dissolution of the β-ala substrate in deionized water then resulted in the complete transfer of the film. The transferred thin films on Cytop were thermally annealed in dry N_2 at 45 °C for 1 h to desorb residual water (that would be detrimental to the OFET characteristics) and to promote full adhesion between the dielectric and the thin film. Gold source and drain electrodes of different widths ($300 \leq W \leq 1000$ μm) and spacing (channel length, $25 \leq L \leq 120$ μm) were thermally evaporated onto the RUB thin films under high vacuum ($\approx 10^{-6}$ mbar) through a shadow mask (see Supporting Information Figure S7). The shadow mask was aligned to the crystallographic direction of the thin film using an optical microscope (Nikon Eclipse LV100) equipped with two polarizers, in

order to exploit the highest mobility in the RUB film (known to be along the $[010]_{RUB}$ direction in single crystals).[53] Electrical characterization was performed in air using a Janis ST 500 probe station and a Keithley 4200 semiconductor parameter analyzer equipped with two 4200-PA pre-amplifiers.

Present Address
† Department of Chemical Engineering, Clean Energy Institute, University of Washington, Seattle, Washington 98195, United States.

Supporting Information
Supporting Information is available from the Wiley Online Library or from the author.

Acknowledgements
The authors acknowledge the Scientific Center for Optical and Electron Microscopy ScopeM of the Swiss Federal Institute of Technology (ETHZ), especially Dr. Fabian Gramm. VCH acknowledges a Marie Curie ETH Zürich Postdoctoral Fellowship. The authors acknowledge Dr. Luisa Barba and Dr. Gianmichele Arrighetti (Elettra Synchrotron Facility) for GIXD measurements and Dr. Enrico Fumagalli for GIXD analyses.
The authors acknowledge Fondazione Cariplo (grant no. 2009/2551) and the Swiss National Science Foundation (award no. 200021-140617) for financial support.

Received: ((will be filled in by the editorial staff))
Revised: ((will be filled in by the editorial staff))
Published online: ((will be filled in by the editorial staff))

[1] V. Podzorov, E. Menard, A. Borissov, V. Kiryukhin, J. A. Rogers, M. E. Gershenson, *Phys. Rev. Lett.* **2004**, *93*, 086602.

[2] H. Najafov, B. Lee, Q. Zhou, L. C. Feldman, V. Podzorov, *Nat. Mater.* **2010**, *9*, 938.

[3] D. Braga, G. Horowitz, *Adv. Mater.* **2009**, *21*, 1473.

[4] H. H. Fong, S. K. So, W. Y. Sham, C. F. Lo, Y. S. Wu, C. H. Chen, *Chem. Phys.* **2004**, *298*, 119.

[5] D. Käfer, L. Ruppel, G. Witte, C. Wöll, *Phys. Rev. Lett.* **2005**, *95*, 166602.

[6] D. Käfer, G. Witte, *Phys. Chem. Chem. Phys.* **2005**, *7*, 2850.

[7] Y. Chen, I. Shih, *Appl. Phys. Lett.* **2009**, *94*, 083304.

[8] M. Haemori, J. Yamaguchi, S. Yaginuma, K. Itaka, H. Koinuma, *Jpn. J. Appl. Phys.* **2005**, *44*, 3740.

[9] Z. Li, J. Du, Q. Tang, F. Wang, J.-B. Xu, J. C. Yu, Q. Miao, *Adv. Mater.* **2010**, *22*, 3242.

[10] C. Du, W. Wang, L. Li, H. Fuchs, L. Chi, *Org. Electron.* **2013**, *14*, 2534.

[11] S.-W. Park, S. H. Jeong, J.-M. Choi, J. M. Hwang, J. H. Kim, S. Im, *Appl. Phys. Lett.* **2007**, *91*, 033506.

[12] H. M. Lee, H. Moon, H.-S. Kim, Y. N. Kim, S.-M. Choi, S. Yoo, S. O. Cho, *Org. Electron.* **2011**, *12*, 1446.

[13] H. Wang, F. Zhu, J. Yang, Y. Geng, D. Yan, *Adv. Mater.* **2007**, *19*, 2168.

[14] X. Qian, T. Wang, D. Yan, *Org. Electron.* **2013**, *14*, 1052.

[15] A. Koma, *Thin Solid Films* **1992**, *216*, 72.

[16] C.-H. Lee, T. Schiros, E. J. G. Santos, B. Kim, K. G. Yager, S. J. Kang, S. Lee, J. Yu, K. Watanabe, T. Taniguchi, J. Hone, E. Kaxiras, C. Nuckolls, P. Kim, *Adv. Mater.* **2014**, *26*, 2812.

[17] X. Zeng, L. Wang, L. Duan, Y. Qiu, *Cryst. Growth Des.* **2008**, *8*, 1617.

[18] W.-S. Hu, S.-Z. Weng, Y.-T. Tao, H.-J. Liu, H.-Y. Lee, *Org. Electron.* **2008**, *9*, 385.

[19] M. Campione, M. Moret, L. Raimondo, A. Sassella, *J. Phys. Chem. C* **2009**, *113*, 20927.

[20] L. Raimondo, E. Fumagalli, M. Moret, M. Campione, A. Borghesi, A. Sassella, *J. Phys. Chem. C* **2013**, *117*, 13981.

[21] M. Campione, *J. Phys. Chem. C* **2008**, *112*, 16178.

[22] A. Sassella, L. Raimondo, M. Campione, A. Borghesi, *Adv. Mater.* **2013**, *25*, 2804.

[23] E. Papavinasam, S. Natarajan, N. C. Shivaprakash, *Int. J. Pept. Protein Res.* **1986**, *28*, 525.

[24] S. Trabattoni, M. Moret, M. Campione, L. Raimondo, A. Sassella, *Cryst. Growth Des.* **2013**, *13*, 4268.

[25] T. L. McMeekin, E. J. Cohn, J. H. Weare, *J. Am. Chem. Soc.* **1936**, *58*, 2173.

[26] H. Yanagi, T. Morikawa, S. Hotta, *Appl. Phys. Lett.* **2002**, *81*, 1512.

[27] Y.-Y. Noh, J.-J. Kim, Y. Yoshida, K. Yase, *Adv. Mater.* **2003**, *15*, 699.

[28] O. D. Jurchescu, A. Meetsma, T. T. M. Palstra, *Acta Crystallogr. Sect. B* **2006**, *62*, 330.

[29] S. Tavazzi, L. Silvestri, M. Campione, A. Borghesi, A. Papagni, P. Spearman, A. Yassar, A. Camposeo, D. Pisignano, *J. Appl. Phys.* **2007**, *102*, 023107.

[30] L. Raimondo, M. Moret, M. Campione, A. Borghesi, A. Sassella, *J. Phys. Chem. C* **2011**, *115*, 5880.

[31] A. Sassella, M. Campione, A. Borghesi, *Riv. Nuovo Cim.* **2008**, *31*, 457.

[32] M. Campione, A. Sassella, M. Moret, A. Papagni, S. Trabattoni, R. Resel, O. Lengyel, V. Marcon, G. Raos, *J. Am. Chem. Soc.* **2006**, *128*, 13378.

[33] M. Moret, A. Borghesi, M. Campione, E. Fumagalli, L. Raimondo, A. Sassella, *Cryst. Res. Technol.* **2011**, *46*, 827.

[34] S. C. B. Mannsfeld, K. Leo, T. Fritz, *Phys. Rev. Lett.* **2005**, *94*, 056104.

[35] T. Haber, R. Resel, A. Thierry, M. Campione, A. Sassella, M. Moret, *Phys. E* **2008**, *41*, 133.

[36] L. Pastero, D. Aquilano, M. Moret, *Cryst. Growth Des.* **2012**, *12*, 2306.

[37] C. Simbrunner, *Semicond. Sci. Technol.* **2013**, *28*, 053001.

[38] M. Campione, L. Raimondo, M. Moret, P. Campiglio, E. Fumagalli, A. Sassella, *Chem. Mater.* **2009**, *21*, 4859.

[39] K. Willa, R. Häusermann, T. Mathis, A. Facchetti, Z. Chen, B. Batlogg, *J. Appl. Phys.* **2013**, *113*, 133707.

[40] W. L. Kalb, T. Mathis, S. Haas, A. F. Stassen, B. Batlogg, *Appl. Phys. Lett.* **2007**, *90*, 092104.

[41] M. E. Gershenson, V. Podzorov, A. F. Morpurgo, *Rev. Mod. Phys.* **2006**, *78*, 973.

[42] T. J. Richards, H. Sirringhaus, *J. Appl. Phys.* **2007**, *102*, 094510.

[43] D. Braga, G. Horowitz, *Appl. Phys. A* **2009**, *95*, 193.

[44] G. Horowitz, R. Hajlaoui, D. Fichou, A. El Kassmi, *J. Appl. Phys.* **1999**, *85*, 3202.

[45] R. J. Chesterfield, J. C. McKeen, C. R. Newman, P. C. Ewbank, D. A. Da Silva Filho, J. L. Brédas, L. L. Miller, K. R. Mann, C. D. Frisbie, *J. Phys. Chem. B* **2004**, *108*, 19281.

[46] V. Podzorov, S. E. Sysoev, E. Loginova, V. M. Pudalov, M. E. Gershenson, *Appl. Phys. Lett.* **2003**, *83*, 3504.

[47] C. Somaschini, S. Bietti, A. Fedorov, N. Koguchi, S. Sanguinetti, *Nanoscale Res. Lett.* **2010**, *5*, 1897.

[48] T. Akiyama, Y. Nakano, H. Kazama, Y. Iizuka, H. Fujiyasu, *Thin Solid Films* **1992**, *214*, 104.

[49] G. M. Morris, D. S. Goodsell, R. S. Halliday, R. Huey, W. E. Hart, R. K. Belew, A. J. Olson, *J. Comput. Chem.* **1998**, *19*, 1639.

[50] M. L. P. Price, D. Ostrovsky, W. L. Jorgensen, *J. Comput. Chem.* **2001**, *22*, 1340.

[51] W. L. Jorgensen, D. S. Maxwell, J. Tirado-Rives, *J. Am. Chem. Soc.* **1996**, *118*, 11225.

[52] A. J. Stone, A. Dullweber, O. Engkvist, E. Fraschini, M. P. Hodges, A. W. Meredith, D. R. Nutt, P. L. A. Popelier, D. J. Wales, *Orient: A Program for Studying Interactions between Molecules*, University Of Cambridge, **2002**.

[53] V. C. Sundar, J. Zaumseil, V. Podzorov, E. Menard, R. L. Willett, T. Someya, M. E. Gershenson, J. A. Rogers, *Science* **2004**, *303*, 1644.

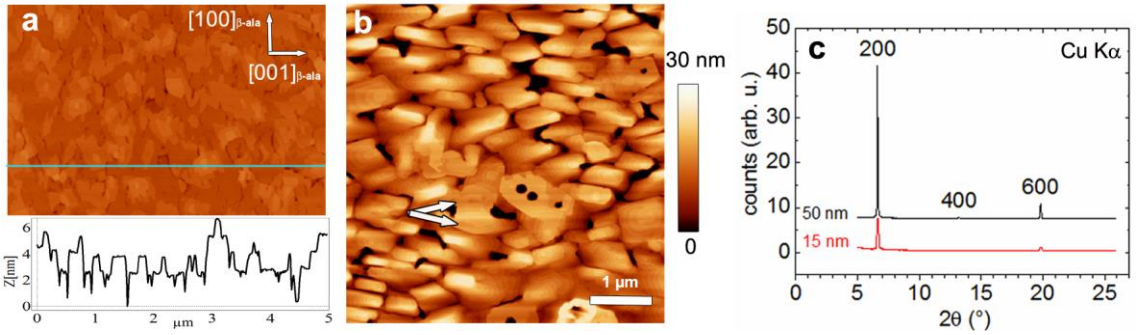

Figure 1. AFM topographic images of RUB films grown on β-ala(010): (a) 5 nm thick film; the inset represents the cross-sectional profile along the light blue line. The crystallographic directions of the substrate surface are indicated on the top right of the panel. (b) 50 nm thick film; the white arrows indicate the elongation directions of the pyramidal islands. (c) XRD specular scans collected on 15 nm (red) and 50 nm (black) thick RUB films grown on β-ala(010) and wet-transferred onto a Si(100) substrate.

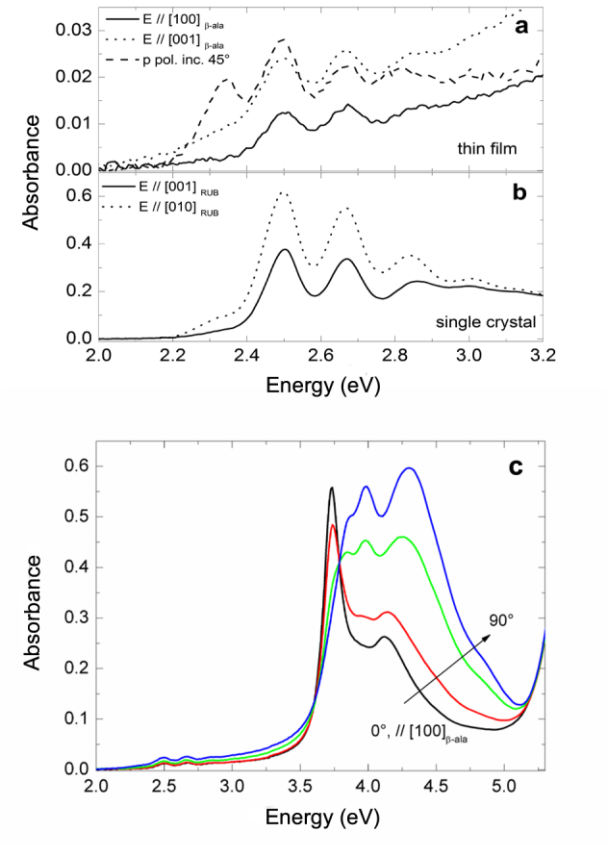

Figure 2. (a) Absorbance spectra of a 5 nm thick RUB film grown on β-ala(010). The electric field of the incident beam is parallel to $[100]_{\beta\text{-ala}}$ (full line) and $[001]_{\beta\text{-ala}}$ (dotted line). The dashed spectrum was collected at 45° incidence under p-polarization. (b) Absorbance spectra of a (100)-oriented orthorhombic RUB single crystal of ≈500 nm thickness, collected at normal incidence. The electric field of the incident beam is parallel to $[001]_{RUB}$ (full line) and $[010]_{RUB}$ (dotted line). (c) Extended absorption spectra of the same 5 nm thick RUB film with the electric field of the incident beam varying from 0° (parallel to $[100]_{\beta\text{-ala}}$, black curve) to 90° (parallel to $[001]_{\beta\text{-ala}}$, blue curve). All spectra are shifted to zero absorbance at 2.0 eV for a better comparison.

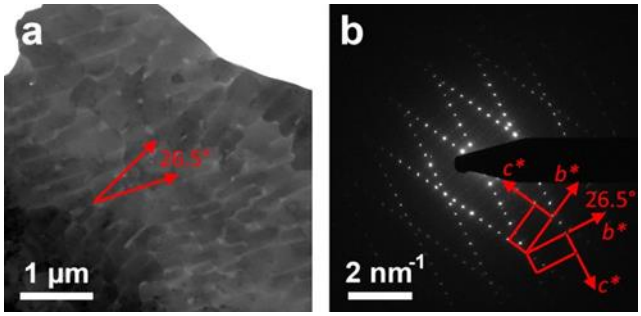

Figure 3. (a) Bright-field TEM image of the same film in Figure 1b after wet-transfer onto a copper TEM grid. Red arrows indicate the elongation directions of the crystalline domains. (b) SAED obtained on the sample in (a), showing the presence of two crystal domains rotated by 26.5° relative to one another.

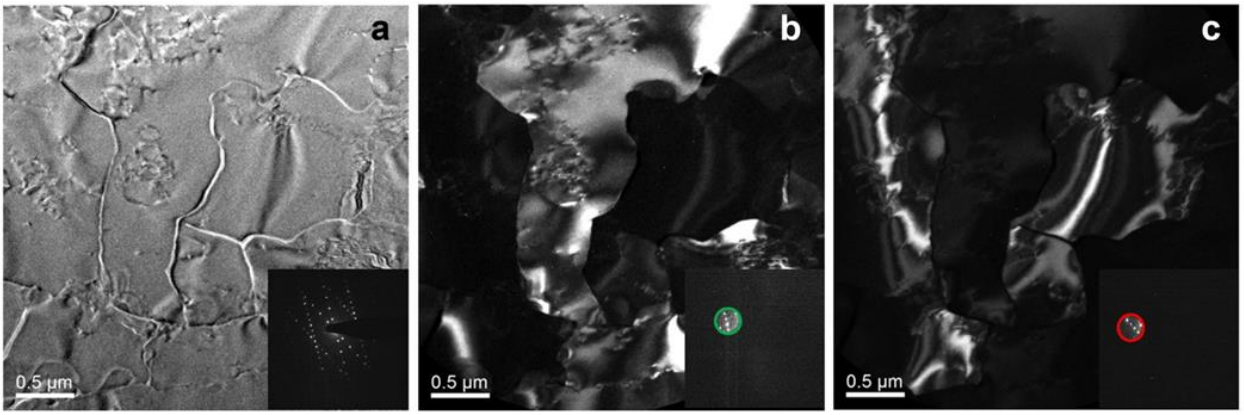

Figure 4. (a) Representative bright-field TEM image and corresponding electron diffraction pattern (inset) of a RUB thin film. (b) Apertured dark-field TEM images formed by selecting diffraction spots corresponding to one domain orientation (green circle) or (c) the other one (red circle).

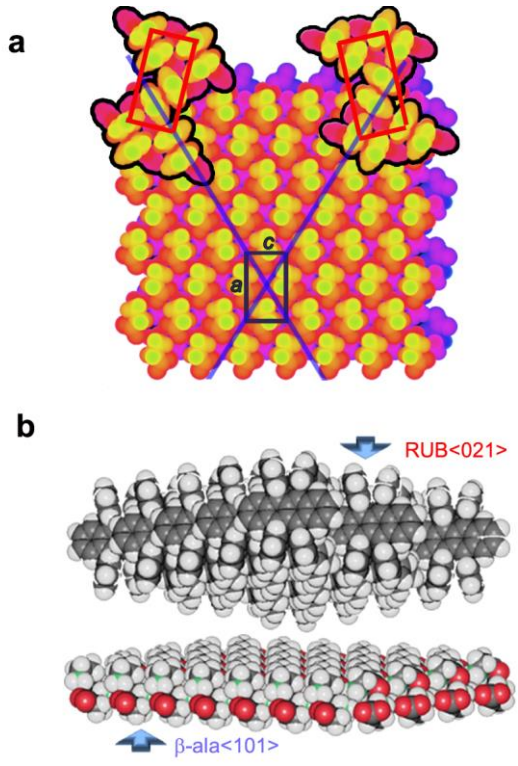

Figure 5. (a) Top-view model of two RUB domains epitaxially grown on β-ala(010), displayed with a depth-dependent color scale; the RUB unit cells are shown in red and the β-ala cell in pale blue. For the sake of clarity only the most abundant domains are reported. (b) Side-view structural model of an epitaxial RUB domain on β-ala(010) showing registry between the corrugations of the $(012)_{RUB}$ and $(101)_{\beta\text{-ala}}$ planes.

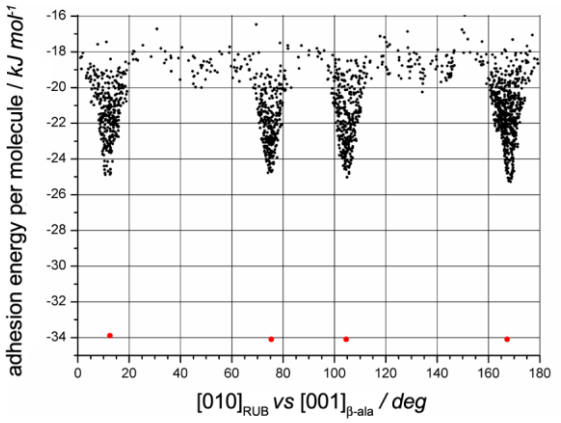

Figure 6. Adhesion energy calculated for a cluster of 16 RUB molecules in the overlayer vs the azimuthal angle. Data points in black color are from the genetic algorithm runs; data points in red color arise from full energy minimization.

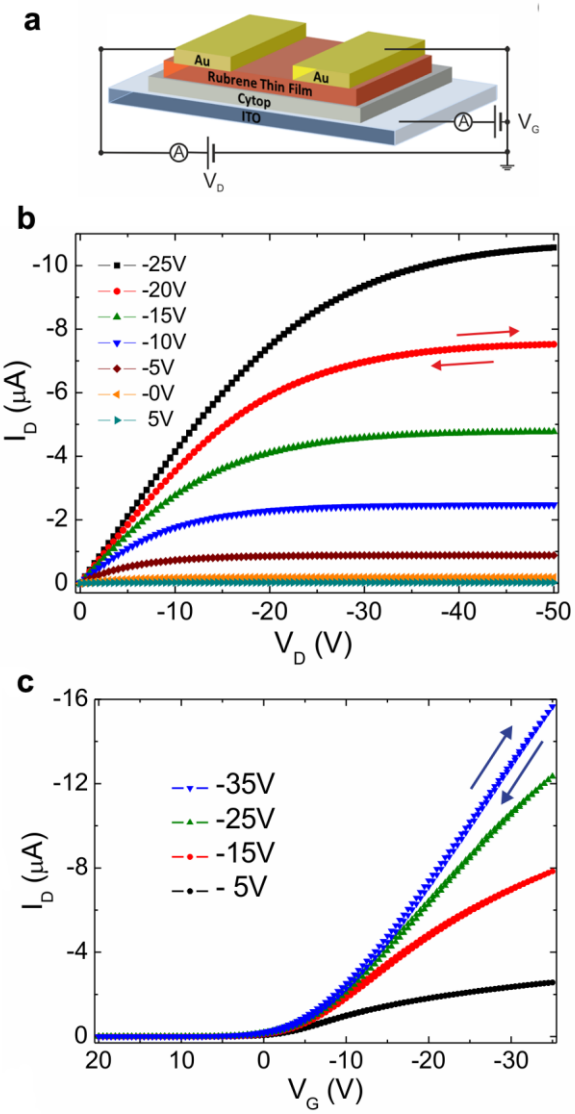

Figure 7. (a) Schematic of a RUB OFET. (b) Drain current (I_D) versus drain voltage (V_D) at different negative gate voltages (output characteristics). (c) I_D-V_G characteristics at different V_D (transfer characteristics) for W = 570 μm and L = 120 μm; the thickness of the dielectric is ≈380 nm.

Table of Contents

β-alanine(010) single crystals are selected as the proper substrate to grow millimeter-sized, orthorhombic rubrene(100) crystalline films exploiting organic epitaxy. The water solubility of β-alanine substrate and the high crystalline quality of RUB thin films allow for the wet-transfer of the semiconductor overlayer onto Cytop and the fabrication of working OFET.

Keywords: rubrene, organic epitaxy, β-alanine, crystalline thin films, wet-transfer

*Silvia Trabattoni *, Luisa Raimondo, Marcello Campione, Daniele Braga, Vincent C. Holmberg†, David J. Norris, Massimo Moret, Andrea Ciavatti, Beatrice Fraboni, Adele Sassella*

Substrate Selection for Full Exploitation of Organic Semiconductor Films: Epitaxial Rubrene on β-alanine Single Crystals

ToC figure

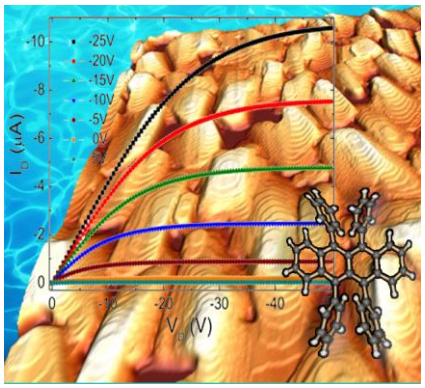

Supporting Information

Click here to download Supporting Information: Supporting Information.doc